Magnetic phase diagram of the $UFe_{1-x}Ni_xAl$ system

R. Troć, V. H. Tran, F. G. Vagizov,* and H. Drulis

W. Trzebiatowski Institute for Low Temperature and Structure Research, Polish Academy of Sciences, 50-950 Wrocław, Poland
(Received 19 January 1994; revised manuscript received 29 August 1994)

Measurements of the lattice parameter (a,c), magnetic susceptibility, magnetization, electrical resistivity, and Mössbauer effect were performed on polycrystalline samples of $UFe_{1-x}Ni_xAl$ solid solutions in the $0 < x \leq 1.0$ composition range. The lattice-parameter variation with x was found to be quite unusual. It appears that at $x \approx 0.3$ the $a(x)$ and $c(x)$ functions go through a sharp cusp; with a maximum value for $a(x)$ and a minimum value for $c(x)$. The susceptibility and magnetization show a systematic increase in magnetic correlation effects with growing Ni substitution, which for the $0.35 < x < 0.8$ samples leads finally to the occurrence of spontaneous ferromagnetism. The maximum Curie temperature and saturation moment are achieved for $x = 0.5$. This behavior has been confirmed by the Mössbauer-effect study performed in the temperature range 13–300 K. Moreover, this study undoubtedly indicates that the Ni substitution is preferential and initially takes place mainly at the $(1b)$ sites. This finding and the increase in the total electron concentration by about 1 electron/f.u. caused by the Ni substitution are primarily responsible for inducing the ferromagnetic properties around $x = 0.5$ in the $UFe_{1-x}Ni_xAl$ alloys. Starting with the $x = 0.9$ composition, an antiferromagnetic correlation develops and a stable antiferromagnetic state is reached for UNiAl with $T_N = 19-23$ K. The Debye temperature for the selected $x = 0.5$ sample, being $\Theta_D = 300$ K, was also estimated from the temperature-dependent Mössbauer-effect data.

I. INTRODUCTION

The Fe_2P-Type uranium ternary compounds of the formula UTM (T is a transition metal and M is a p-electron metal) constitute one of largest isostructural groups of uranium intermetallics, being widely studied in recent years.

A study of the physical properties of the Fe_2P-type subgroup provides a unique possibility of investigating the systematic changes of the $5f$-electron behavior through the variation of T or/and M components, keeping the general geometry of the atom arrangement in the crystal lattice unchanged. Hence, the observed physical properties can be correlated with the electronic structure, reflecting especially the varying $5f$-ligand hybridization effect, which leads to more or less broadened $5f$ bands located near the Fermi energy E_F.

It is obvious that the strongest hybridization limit is expected for the lowest populated nd states of a transition metal constituting a given UTM compound, e.g., Fe, Ru, and possibly Os, elements belonging to the same column in the periodic table. Therefore, not unexpectedly, UFe (Al, Ga) (Refs. 1,2) and URu(Al,Ga) (Ref. 1) were found to be either enhanced Pauli paramagnets or/and spin-fluctuating systems. Moreover, for the two former compounds no anisotropy in the magnetization could be detected.[1]

In turn, UNiAl, which is also one of the more than 25 ternary Fe_2P-type uranium compounds known so far, orders antiferromagnetically below 19 K,[3] with a rather complex magnetic structure, being unresolved up to date.[4] Due to a fairly high value for the electronic specific-heat coefficient $\gamma(0) = 164$ mJ mol^{-1}K^{-2}, the low magnetic entropy at T_N,[5] and the rapid suppression

of long-range magnetic order by other-element substitution,[6] UNiAl has been described as an itinerant antiferromagnet.[3]

The self-constituent linear muffin-tin orbital (LMTO) band calculations made for UFeAl (Ref. 7) have demonstrated that the Fermi level lies in between the occupied $3d$ band and the unoccupied $5f$ band, and therefore the density of states (DOS) at E_F is quite low [$\gamma(0) = 25$ mJ mol^{-1}K^{-2}],[1] not satisfying the Stoner criterion for long-range magnetism. In the case of UNiAl (two more valence electrons), Gasche et $al.$[7] stated that the Fermi level rises up into the $5f$ band, and this becomes a sufficient condition for yielding the magnetic state. Also, a photoemission experiment has shown that the $3d$ band becomes narrower and is pushed towards higher binding energies of about -2 eV, while the $5f$ states remain in the vicinity of E_F.[8]

In this paper we present our studies of the magnetic, electrical-resistivity, and Mössbauer-effect behavior of the pseudoternary system $U(Fe_{1-x}Ni_x)Al$, where $x = 0.05-1.0$. Previously we studied similar properties for UFeAl.[2]

II. EXPERIMENTAL DETAILS

Polycrystalline samples of $UFe_{1-x}Ni_xAl$ with $0 \leq x \leq 1.0$ were prepared by arc-melting stoichiometric quantities of high-purity uranium and 99.99%-pure other constituents under an argon atmosphere. The samples rich in Ni were isotopically enriched with 90% ^{57}Fe metal.

After arc melting the samples were sealed in evacuated quartz ampoules and annealed for two weeks at 650 °C. For x-ray and Mössbauer-effect measurements, the brittle

buttons were crushed in a glovebox under a protective argon atmosphere in order to make fine powders.

All the x-ray patterns taken for many samples of the above solid solutions (except for UFeAl) were identified as showing only the hexagonal Fe_2P-type structure. From all possible impurity phases, such as UFe_2, α-U, and UO_2, the presence of only very small quantities of the latter phase could sometimes be detected, so that all the specimens were essentially single phased.

Magnetic-susceptibility measurements, continuously recorded with increasing temperature, were performed using a Cahn RH electronic balance over the temperature range 4.2–300 K.

In order to check the samples for any ferromagnetic impurities, especially for the presence of extraneous α-Fe or/and UFe_2 ($T_C = 150$–160 K), we measured the susceptibility χ at several magnetic fields between 0.05 and 0.6 T, both at room temperature (RT) and at 4.2 K.

The temperature and field dependence of the magnetization at low temperatures and in magnetic fields up to 4 T were also measured for the ferromagnetic samples.

Electrical-resistivity measurements for the $x = 0.3$, 0.5, and 0.9 samples were carried out by a standard dc four-probe technique in the temperature range 4.2–300 K. Cu wires were spot welded to the samples, shaped as bars with the dimensions of $0.5 \times 1.0 \times 3.0$ mm.[3] However, their high brittleness prevents getting high-accuracy results in practice.

Mössbauer-effect measurements were carried out from 13 to 295 K, using a conventional constant-acceleration spectrometer POLON with [57]Co in a chromium matrix as the source. A metallic-iron foil at RT was used for velocity calibration of the Mössbauer spectrometer. In order to obtain thin and uniform absorbers for measurements and to avoid texture problems, the investigated compounds were finely ground and mixed with boron nitride. Least-squares computer programs were used to derive from Mössbauer absorption spectra the values of the hyperfine interaction parameters and the distribution of the Fe atoms between nonequivalent crystallographic positions.

III. RESULTS

A. Structural details

In the Fe_2P-type unit cell, the U, T, and M atoms in the UTM systems are arranged in M-$T_{II}(2c)$ ($z=0$) and U-$T_I(1b)(z=\frac{1}{2})$ planar layers, stacked perpendicular to the c axis. Here $T_I(1b)$ and $T_{II}(2c)$ denote two transition-metal sites in the unit cell, which occupy the phosphorus sites. The U and M atoms are ordered at the (3g) and (3f) positions, respectively. These two different atomic layers are shown in Fig. 1. The uranium atoms in this crystal structure have the highest coordination number (CN), 15. The U-U separation within the layer is connected with the lattice parameter a by the expression $d_{U-U} \approx 0.53a$ and this distance in UFeAl and UNiAl is 3.50 and 3.54 Å, respectively. The interlayer U-U separation is larger than that within the layer by about 0.6 Å.

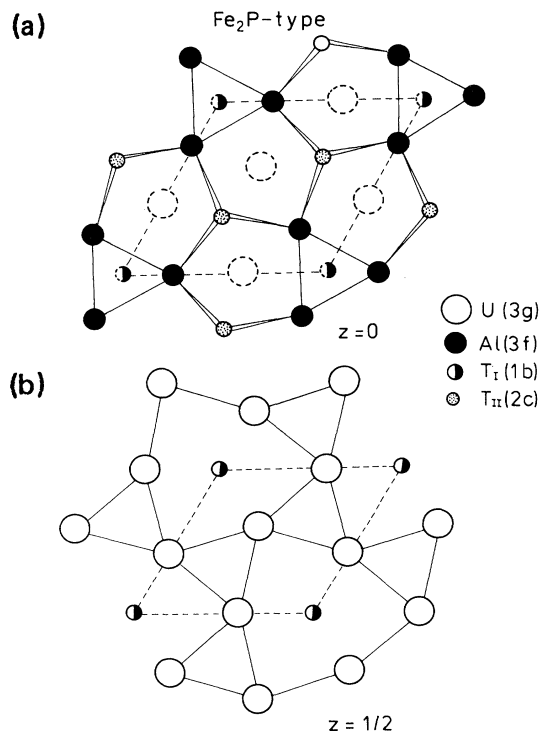In view of the small difference in the lattice parameters

FIG. 1. Projection of the crystal structure of Fe_2P type along the c axis in the basal planes: (a) U-T_I, and (b) Al-T_{II}.

of the respective unit cells of the Fe- and Ni-based compounds, one would expect their rather smooth change in the solid solutions $UFe_{1-x}Ni_xAl$. It appears, however, that this change is dramatic. The results obtained on numerous samples are presented in Fig. 2 in the form of
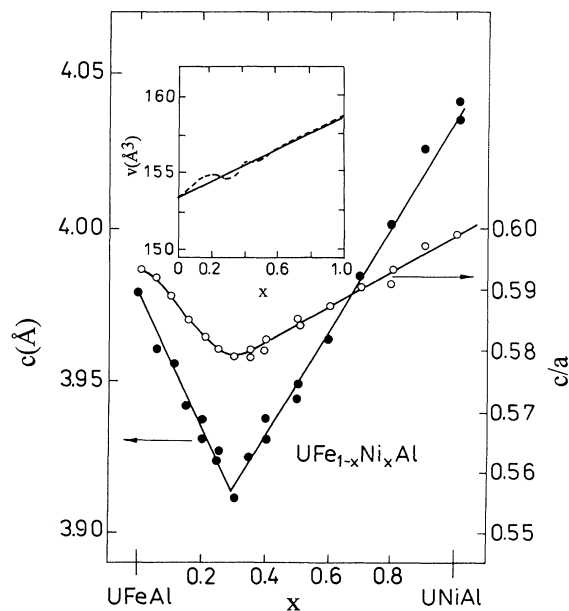

FIG. 2. Lattice parameter c and the ratio c/a as a function of Ni concentration x in the $UFe_{1-x}Ni_xAl$ alloys. Inset: unit-cell volume V as a function of x.

the c and c/a variations with increasing Ni content x. As shown in the inset of this figure, the unit-cell volume is rather linear in x.

In order to explain this dramatic change in the lattice parameters near $x \approx 0.3$, the key problem arises about the way of occupancy of the (1b) and (2c) sites in the process of systematic substitution of Fe atoms by the Ni atoms in these solid solutions. This could be done by means of Mössbauer-effect investigations. The results of such investigations we will present later.

B. Magnetic behavior

Figure 3 presents the temperature dependence of the inverses magnetic susceptibility χ^{-1}, for the $0 \le x \le 1$ samples of UFe$_{1-x}$Ni$_x$Al. We have already published the results for UFeAl ($x = 0$) in its two polymorphic structural forms.[2] Here, for completeness, we have only marked in Fig. 3 a very weak temperature dependence of the UFeAl susceptibility. As this figure demonstrates, a small Ni doping causes a more distinct variation of χ^{-1} with temperature, particularly at low temperatures. A further increase in x leads to the appearance of increased curvature of $\chi^{-1}(T)$ at higher temperatures and an S
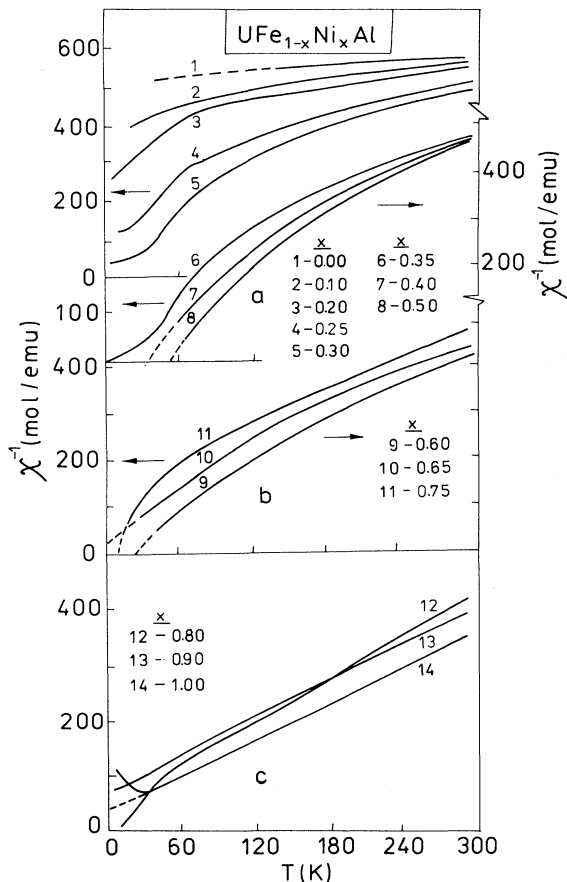
shape of $\chi^{-1}(T)$ at lower temperatures. The latter behavior indicates a growing magnetic interaction when more and more Fe atoms are exchanged by the Ni atoms in the alloy. Assuming for the susceptibility at higher temperatures a modified Curie-Weiss dependence, we found the values of Θ_p and $\mu_{\rm eff}$/U atom, which we have plotted against x in Figs. 4 and 5, respectively.

For Fe-rich alloys especially both these values have only informative meaning. For example, as follows from Fig. 4, Θ_p changes rapidly from extremely negative values at small x, reaching $\Theta_p \approx 0$ K at $x \approx 0.3$. At the same time, $\mu_{\rm eff}$ decreases from unrealistic value of $\approx 4.5\mu_B$ for $x = 0.05$ to about $1\mu_B$ for the same composition as above. A further increase in x leads Θ_p first to become positive, then to go through a maximum at $x = 0.5$, and finally, above $x = 0.7$ to become negative again, this time meaning that we are really dealing with the change of the exchange interactions from ferromagnetic to antiferromagnetic character. On the other hand, the $\mu_{\rm eff}$ values for the samples with $x > 0.3$ start to increase linearly (within experimental error) with simultaneous diminishing of the χ_0 values. Finally, for UNiAl the inverse susceptibility vs temperature dependence is almost linear and yields the following magnetic parameters: $\Theta_p = -21$ K, $\mu_{\rm eff} = 2.5\mu_B$, and $\chi_0 = 3.6 \times 10^{-4}$ emu/mol. These data agree more or less with the powder data of other authors,[1] but differ from the results obtained for a single crystal of UNiAl.[5] It appears from the latter data that all the magnetic response of this system is only along the c axis, which leads to a higher value of $\mu_{\rm eff} = 2.9\mu_B$ along this axis, and to a very small contribution of χ_0.[5]
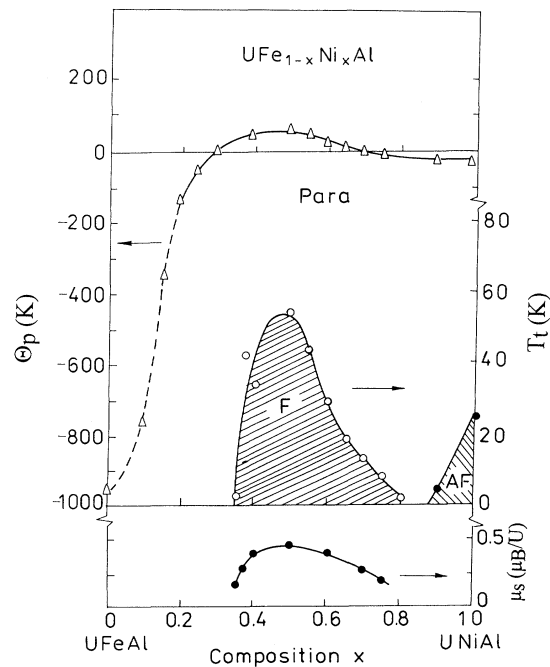

FIG. 3. Inverse magnetic susceptibility χ^{-1} as a function of temperature for the UFe$_{1-x}$Ni$_x$Al samples, where $0 \le x \le 1.0$.

FIG. 4. Magnetic phase diagram of the UFe$_{1-x}$Ni$_x$Al system: transition temperature T_t, paramagnetic Curie temperature Θ_p, and saturation magnetic moment of uranium μ_s as a function of Ni concentration x.
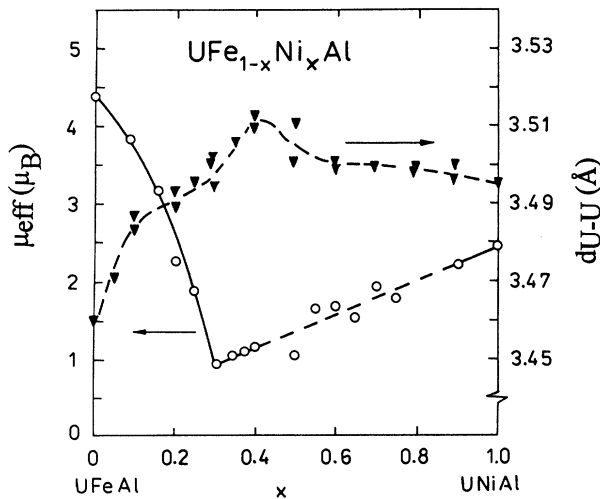
FIG. 5. Effective magnetic moment μ_{eff} per uranium atom and U-U distance d_{U-U} as a function of Ni concentration x in the $UFe_{1-x}Ni_xAl$ system.

The latter means that the Curie-Weiss law is in practice well obeyed by the susceptibility measured parallel to the c axis, $\chi_{\parallel}(T)$.

As already mentioned, Θ_p for $0.35 \le x \le 0.75$ reaches positive values. Therefore ferromagnetic order sets in for these compositions. As one can see from Fig. 6(a), the magnetization expressed in Bohr magnetons for the samples with $x = 0.35$ and 0.75, as well as with $x = 0.4$ and 0.6, exhibits a similar behavior. For the former pair of compositions the magnetization has negative curvature in applied magnetic fields up to 4 T, with a distinct hysteresis. This curve for the latter pair of compositions and for the $x = 0.5$ sample, in general, has a behavior as for the normal actinide ferromagnets, i.e., it reaches the saturation value μ_s in rather high fields of 1–2 T, and shows a relatively large remanence. However, one feature of this curve taken for the compositions $0.35 \le x \le 0.5$ is not

the usual one. This feature can be better seen in Fig. 6(b), where the magnetization is plotted against the field for the samples with $x = 0.4$, 0.5, and 0.6, obtained by separate synthesis. As seen, for the two first samples, the magnetization increases in two steps. Since these measurements were made on powder samples, we leave now this feature of $\mu(B)$ without trying to explain its origin. It is clear that this feature does not occur for the samples with $x > 0.5$. As shown in Fig. 4, the tail of the ferromagnetic behavior extends as far as $x \approx 0.8$. The maximum transition temperature of $T_C = 55$ K is observed for the $x = 0.5$ sample. Also the saturation moment reaches its maximum for the same composition (see Fig. 4). It should be noted that these powder values of μ_s should be multiplied by a factor of 2 in order to get the proper values of the uranium ordered moment in the ferromagnetic region of the solid solutions $UFe_{1-x}Ni_xAl$. Of course, the above statement is valid only in the case of nonmagnetic behavior of Fe and Ni atoms in these solid solutions, as we have assumed.

The compositions with $0.8 < x < 0.9$ do not exhibit a long-range magnetic order. However, it is likely that some kind of short-range magnetic order or spin freezing of the moments exists in this composition range.

As one would expect, the samples with $x > 0.9$ are antiferromagnetic (see the magnetic phase diagram of $UFe_{1-x}Ni_xAl$ displayed in Fig. 4). It is also interesting to point out that the ferromagnetic region of compositions is attributed to the maximum values in the U-U distances. This is clearly shown in Fig. 5. One should however bear in mind that when Ni substitutes for Fe, it introduces two more valence electrons to the solid solutions. Hence the occurrence of the ferromagnetism around the composition $UFe_{0.5}Ni_{0.5}Al$ is indicative of the fact that such behavior can be induced in the alloy by an increase in the total number of the valence electrons by about 1 electron/f.u., assuming simultaneously that the maximum in the U-U distances (Fig. 5), observed just at $x = 0.5$, has a lesser role in the creation of spontaneous magnetization.
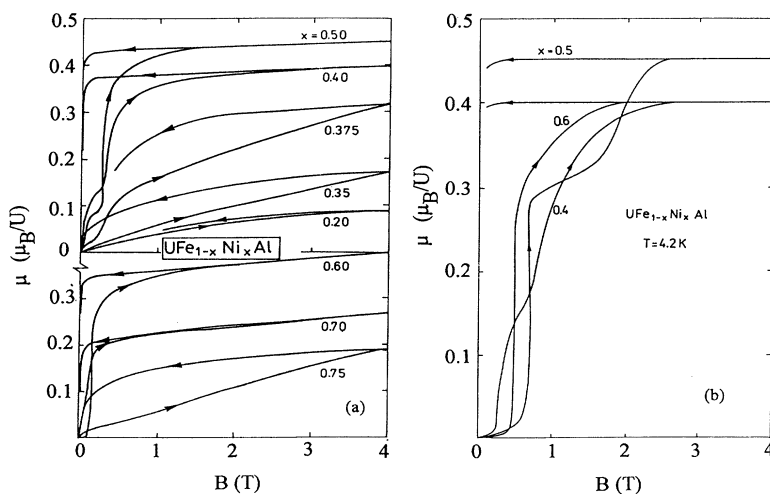

FIG. 6. Magnetization at 4.2 K as a function of applied magnetic field for the $UFe_{1-x}Ni_xAl$ alloys. (a) for $0.2 \le x \le 0.75$, and (b) for samples of different synthesis, with $x = 0.4$, 0.5, and 0.6. Note a two-step magnetization process for the $x = 0.4$ and 0.5 samples.

C. Electrical resistivity

The electrical-resistivity behavior for the sample richest in Fe but being still a completely pure Fe$_2$P-type phase, namely, for UFe$_{0.95}$Ni$_{0.05}$Al, was reported by us previously.[2] The observed S shape and aT^2 dependence at low temperatures of $\rho(T)$ of this phase favored an interpretation that the spin fluctuations with a rather high T_{sf} (magnetic susceptibility is almost independent of temperature) dominate in this phase.

On the other hand, the reported resistivity of UNiAl, measured on single-crystal platelets along the ab plane and along the c direction showed (except in the low-temperature range) a very weak temperature dependence with little anisotropy.[9,10] The observed higher resistivity within the ab plane than along the c direction was attributed by Schoenes et al.[9] to a stronger hybridization of the conduction electrons with the $5f$ electrons, just in the region of the U-(Fe,Ni)$_I$ plane.

In addition, we measured $\rho(T)$ for three compositions with $x = 0.3$, 0.5, and 0.9. The results are shown in Fig. 7. All three curves exhibit almost the same behavior. At the lowest temperatures a shallow minimum occurs. No anomaly, however is seen in $\rho(T)$ or in $d\rho(T)/dT$ (see the inset of Fig. 7) for the magnetically ordered samples, i.e., with $x = 0.5$ and 0.9, near their transition temperatures, marked in Fig. 7 by arrows. However, one should bear in mind that the resistivity results obtained for the polycrystalline samples of the UFe$_{1-x}$Ni$_x$Al solid solutions may not be conclusive, due to the fact that the samples used were extremely brittle. Nevertheless, their character is typical for numerous solid solutions of uranium or cerium intermetallics.

D. Mössbauer effect

Figure 8(a) shows the ^{57}Fe Mössbauer spectra measured at RT for selected compositions of the solid solutions UFe$_{1-x}$Ni$_x$Al. All of them consist of two symmetrical doublets.

A more intensive doublet with a larger quadrupole splitting (QS) corresponds to the Fe atoms occupying the $(2c)$ sites. The doublet having a smaller QS corresponds to the $(1b)$ sites. This difference in the QS values arises from the fact that the environment in the Fe$_2$P-type lattice is more asymmetric around Fe at the $(2c)$ sites than that around Fe at the $(1b)$ sites (see Fig. 1).

The intensity ratio of these doublets measured for the single-phase UFe$_{0.95}$Ni$_{0.05}$Al (see Ref. 2), taken as the ratio of areas under the respective doublets, is $S_{(2c)}/S_{(1b)} \approx 2.14$, as compared to the theoretical value of 2.10. The latter value is found for the case of the full preference of the $(1b)$ sites by Ni.

The structural changes due to the Ni concentration should be reflected in the hyperfine interaction parameters. We have plotted, therefore, the isomer shift (IS) [Fig. 9(a)], and the quadrupole splitting [Fig. 9(b)] (both taken at 13 and 295 K) against the Ni concentration x in the alloys, separately for the structure sites $(1b)$ and $(2c)$. As one can see from this figure, the IS for the $(2c)$ sites (within experimental error) remains unchanged with x, while that for the $(1b)$ sites increases slightly in an opposite way than does the QS [Fig. 9(b)]. Some deviation from linearity for the $x > 0.3$ samples, observed in the variation of both IS and QS with x at 13 K is caused by uncertainties in the measurements (very small occupation of these sites by ^{57}Fe and the possible presence of short-range magnetic order in the $x > 0.3$ samples).

On the other hand, $\Delta_{QS}(x)$ for the $(2c)$ sites alternates distinctly with x at both temperatures and has a positive cusp at $x \approx 0.35$. This correlates well with the concentration variation of the lattice parameter a. On this basis one can conclude that at RT the cusp variation of the $\Delta_{QS}(x)$ function is first of all attributed to the predominant contribution of the lattice, q_{latt}, to the electric field gradient (EFG). Indeed, the first coordination sphere around the Fe (Ni) atom in both sites does not have any other Fe (Ni) atoms, but only U or Al atoms (Fig. 1).

As one can infer from Fig. 8(a), the intensity of the $(1b)$ doublet, i.e., that with a smaller QS, decreases
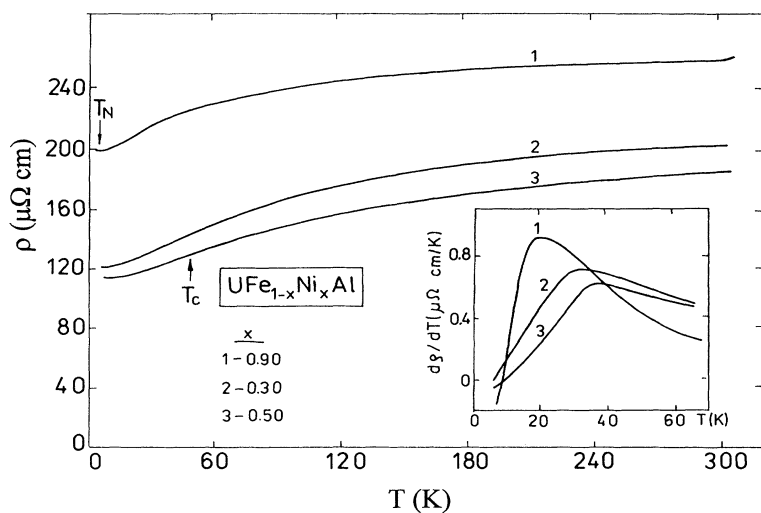

FIG. 7. Electrical resistivity as a function of temperature for UFe$_{1-x}$Ni$_x$Al samples with $x = 0.3$, 0.5, and 0.9. Inset: the derivative $d\rho/dT$ as a function of temperature for these samples.

smoothly with increasing Ni content in the alloy and in practice it becomes undetected for $x > 0.45$. This feature is caused by the fact that the substitution of the larger Fe atom ($R_{Fe} \approx 1.26$ Å) by the smaller Ni atoms ($R_{Ni} \approx 1.24$ Å) takes place first of all at the ($1b$) sites, having smaller space than the ($2c$) sites.

In Fig. 10, the occupancy of the ($1b$) and ($2c$) sites by the Fe atoms, depending on the Ni concentration, inferred from the Mössbauer data, is presented. As seen, the exchange of Fe by Ni at the ($2c$) sites is considerably slower than that at the ($1b$) sites (compare the slopes of the straight lines drawn up to $x \approx 0.5$). In this figure, we have also marked by the dashed and dot-dashed lines the above-mentioned process in these senses of a statistical substitution of the Fe by Ni atoms at both sites and a complete preference of the Ni atoms to occupy the ($1b$) sites up to $x \approx 0.3$, respectively.

In general, the Fe (Ni) occupancy of the structural sites with increasing Ni content shown in Fig. 10 is most re-

sponsible for the observed variation in the lattice parameters (cf. Ref. 11). The only difference is that the sharp cusps observed for the lattice parameters occur somewhat earlier, namely, at $x \approx 0.3$, than the complete filling of the (1) sites by Ni, namely, at $x \approx 0.5$.

In the view of the constant electron density on the U and Al atoms, the variation in the Ni concentration should not necessarily influence the isomer shift. In fact, this prediction is in agreement with our experiment for the ($2c$) sites, but the opposite is true for the ($1b$) sites (Fig. 9). This is probably due to the appreciable dehybridization effect, taking place first all at the ($1b$) sites between the U $5f$ and Fe (Ni) $3d$ states, with increasing Ni concentration.

At low temperatures the ^{57}Fe Mössbauer spectra for the initial and final ranges of Ni concentrations are roughly analogous to those at RT [Fig. 8(b)]. However, the spectra for the samples with $x = 0.4$, 0.5, 0.6 and 0.7 show some distinct differences [compare Fig. 8(b) with
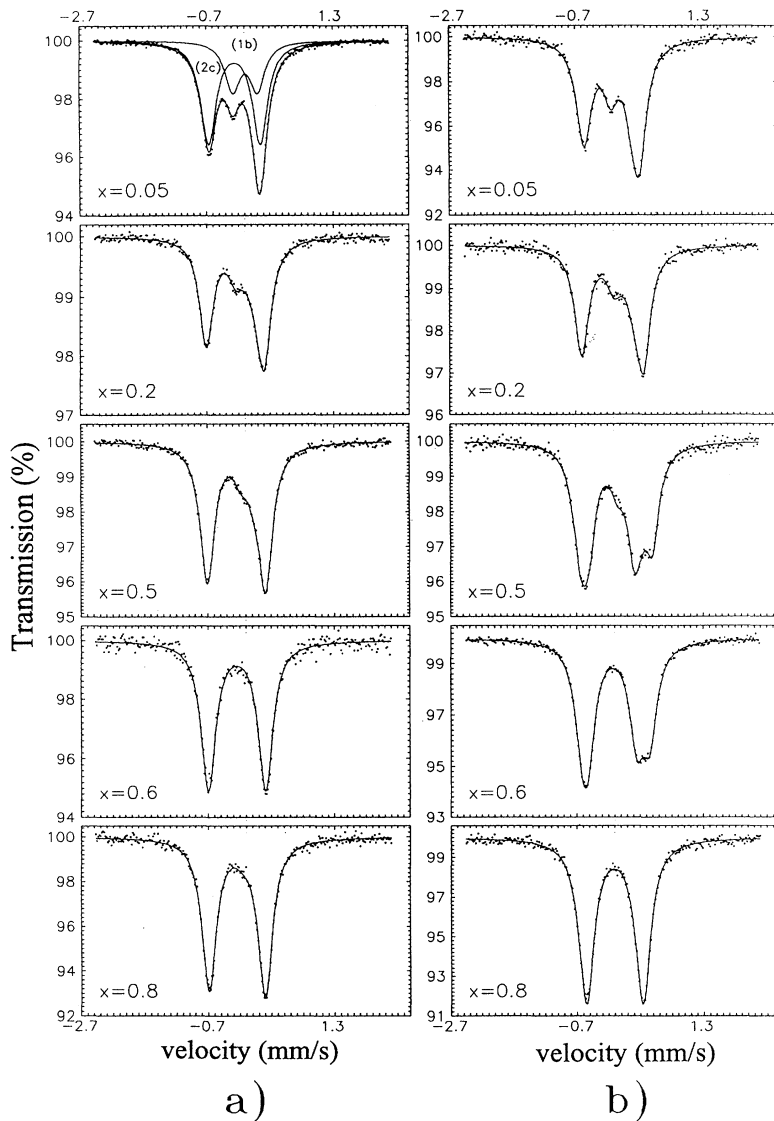

FIG. 8. Mössbauer spectra for the UFe$_{1-x}$Ni$_x$Al samples with $x = 0.05$, 0.2, 0.5, 0.6, and 0.8: (a) at room temperature; (b) at 13 K. At the top solid points, experimental data; solid lines, model-fitted profiles of the Mössbauer spectra, assuming that the Fe atoms are at the two sites ($1b$) and ($2c$).
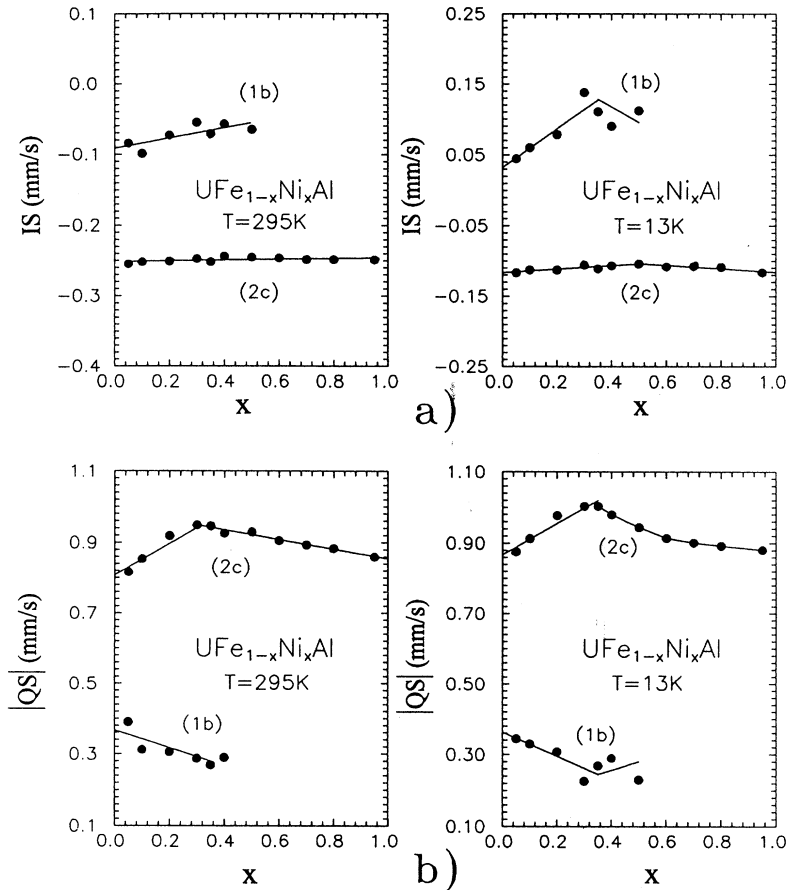
a)   b)

FIG. 9. (a) The isomer shift (IS) relative to α-Fe at 295 and 13 K for Fe at the (1b) and (2c) sites as a function of Ni concentration x. (b) The quadrupole splitting (QS) at 295 and 13 K for Fe at the (1b) and (2c) sites, as a function of Ni concentration x. The lines drawn through the data points are guides for the eye.
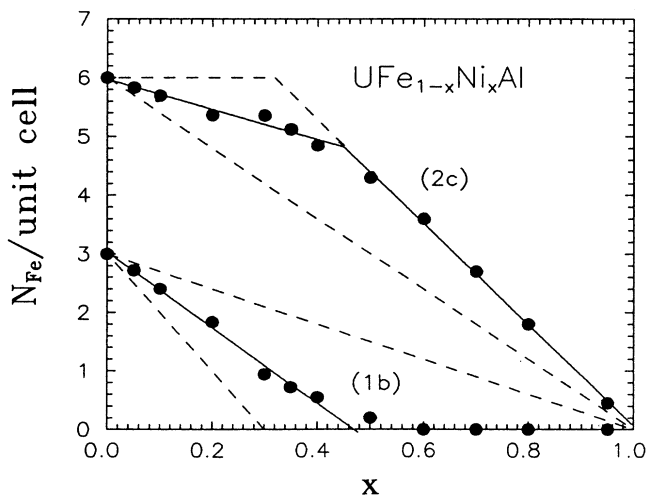

FIG. 10. The number of Fe atoms, N_{Fe}/unit cell, occupying the (1b) and (2c) sites as a function of Ni concentration x. The dashed lines show the case of eventual statistical occupancy of the sites by Fe and Ni atoms, while the dot-dashed lines show an ideal exchange of the Fe atoms by Ni first at the (1b) sites and then, after filling these sites at $x = 0.3$, at the (2c) sites.

Fig. 8(a), for $x = 0.5$ and $x = 0.6$ samples, respectively]. Therefore, for a good approximation of the experimental Mössbauer spectra recorded at 13 K, we have to assume also the presence of nuclear Zeeman interactions in the $0.4 \leq x \leq 0.7$ samples. In Fig. 8(b), the solid line represents the least-squares fitting to the ^{57}Fe Mössbauer spectra of the above compositions [in Fig. 8(b) are shown only the spectra for $x = 0.5$ and 0.6]. Due to a small intensity of the lines corresponding to the Fe atoms at the (1b) sites we have made an assumption that all the Fe nuclei have the same magnetic field, i.e., $H_{\text{hf}}^{(1b)} = H_{\text{hf}}^{(2c)} = H_{\text{hf}}$.

On the other hand, if the small magnetic field is transferred to an iron nucleus from the magnetically ordered uranium sublattice, then owing to the different geometrical surroundings it should be properly assumed that $H_{\text{hf}}^{(1b)} \geq H_{\text{hf}}^{(2c)}$. Unfortunately, the statistical accuracy of our measurements does not allow us to confirm or rule out the above assumption.

In Fig. 11 we demonstrate the dependence of the hyperfine magnetic field at the Fe nuclei, H_{hf} on the Ni concentration. It is clear that this dependence is related to that found from the magnetization (compare with Fig. 4).

The lack of the nuclear Zeeman effect in the Mössbauer spectra of the Ni-rich samples, as, for exam-
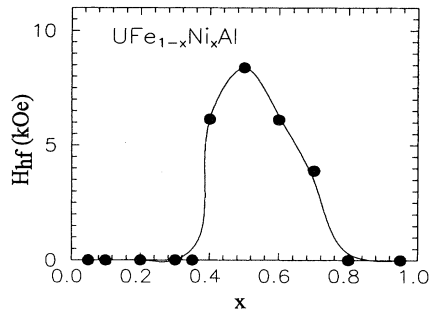
FIG. 11. Hyperfine field H_{hf} as a function of Ni concentration x. Note a similar behavior of the H_{hf} vs x curve to that found in the magnetization study (compare with Fig. 4).

ple, for the $UFe_{0.05}Ni_{0.95}Al$ alloy, is obviously attributed to the antiferromagnetic ordering of the uranium sublattices and mutual compensation of the transferred magnetic fields, originating from the moments oriented up and down. Unfortunately, the proper magnetic structure of UNiAl has not been resolved so far.[4]

In Fig. 12 the hyperfine magnetic field H_{hf} is plotted against temperature for the $x = 0.4$, 0.5, and 0.6 samples. The arrows marked in this figure represent the Curie temperatures found from the magnetization study. It should be emphasized that, in spite of the low accuracy in the determination of the H_{hf} vs T curves, a fairly good agreement in the T_C values has been achieved in the

Mössbauer and magnetization studies.

In analyzing the isomer-shift results found from the Mössbauer data recorded at 13 K [Fig. 8(b)], we see that the most pronounced effect is that observed for the Fe($1b$) atoms, while in the case of the Fe($2c$) atoms, only a slight change in the slope of $\delta_{IS}(x)$ is seen at $x \approx 0.5$ [Fig. 9(a)]. Such a behavior of the IS at low temperatures can be accounted for by a change in the electron density of the atoms at the ($1b$) sites, brought about by the exchange of Fe by Ni. The latter atom introduces two more electrons and strongly influences the process of f-d dehybridization with increasing x at the ($1b$) sites, while this process almost does not take place in the case of the Fe/Ni exchange at the ($2c$) sites (see discussion below).

In connection with the special character of the IS variation of Fe at its ($1b$) sites we have performed studies of the temperature dependence of the hyperfine interaction
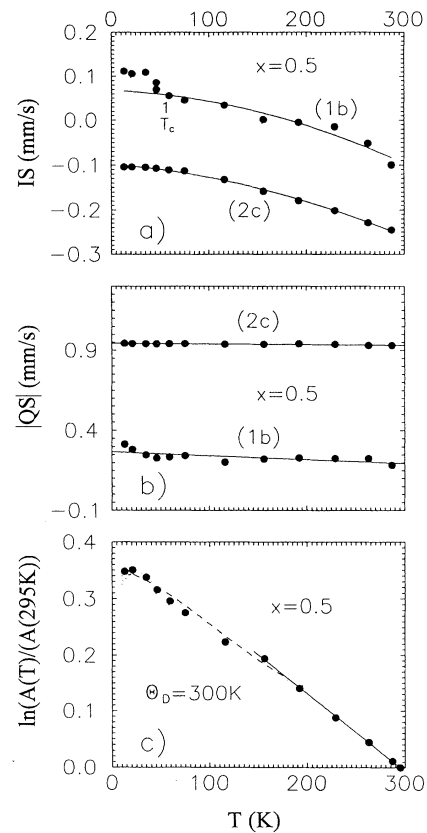
FIG. 13. Hyperfine parameters of Fe in the ($1b$) and ($2c$) sites for $UFe_{0.5}Ni_{0.5}Al$. Upper plot: temperature dependence of the isomer shift (IS). The data can be fitted with reasonable accuracy by the functions which are connected with the Debye integral for $\Theta_D = 300$ K (see text). Middle plot: temperature dependence of the Mössbauer quadrupole splitting, (QS). Note that, within the experimental error, the QS for both Fe sites remains unchanged with temperature. Bottom plot: temperature variation of $\ln[A(T)/A(295\ K)]$, where A is Mössbauer absorption area. The fit for $\Theta_D = 300$ K describes the data from RT to about 150 K, below which the softening of the lattice occurs.
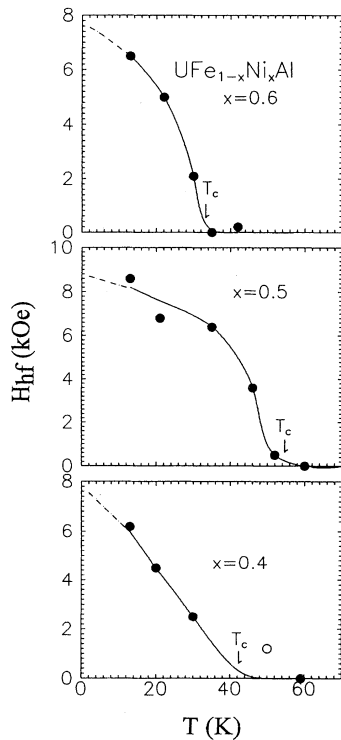

FIG. 12. Hyperfine field H_{hf} as a function of temperature for the compositions $x = 0.4$, 0.5, and 0.6. The arrows show the T_C values found in the magnetic study.

parameters and attempted to determine the Debye temperature Θ_D for one selected composition of the UFe$_{1-x}$Ni$_x$Al alloys, namely, for the alloy with $x = 0.5$. In Fig. 13 are shown the result of such investigations. Details were given in a previous paper.[2] At the bottom of this figure the temperature dependence of the logarithm of the reduced Mössbauer absorption areas $A(T)$ is shown, which is proportional to the recoil-free fraction. The solid straight line is a least-squares fit to the Debye model above 150 K. This fit yields $\Theta_D = 300$ K. The upper plot of Fig. 13 gives the temperature dependences of the isomer shift, $\delta_{IS}(T)$, for both the (1b) and (2c) sites of the Fe atoms. In general, both sets of data can be fitted with a reasonable accuracy to a second-order Doppler shift, characteristic of a Debye temperature $\Theta_D \approx 300$ K. However, as this figure demonstrates, the temperature variation of isomer shift for the (1b) site is well reproduced only at temperatures above T_C ($= 55$ K). In the range of low temperatures one observes a considerable deviation from a smooth curve. This deviation, as we have already mentioned above, is likely associated with a change in the electron-density distribution in the ordered state.

As the middle plot of Fig. 13 indicates, the QS parameters appear to be unchanged with temperature for both crystallographic sites (1b) and (2c).

IV. DISCUSSION

As we pointed out in a previous paper,[2] the exchange-enhanced Pauli paramagnetism of UFeAl with the RT susceptibility value of about 1.6×10^{-3} emu/mol U is predominantly associated with the f-electron character of the band at E_F, thereby contradicting the result of Gasche et al.[7] Our result is remarkably different, for example, from the case of UFe$_2$, which is mainly a 3d ferromagnet.[12] We think that this difference arises mainly from the fact that the 3d band of Fe in UFeAl is filled to large extent by a transfer of charges from uranium, being a more electropositive metal. This means that the almost filled 3d band after this transfer is pushed away from the Fermi level, while the 5f level remains still strongly pinned to this level. Such a picture is in general agreement with photoemission experiments (see, e.g., Ref. 13). Also ultraviolet photoemission spectroscopy (UPS) valence-band measurements, made for binary glass systems U$_{100-x}$Fe$_x$ where $x \leq 50$,[14] have revealed that the narrow band observed near E_F is due to the 5f electrons, while the 3d-electron band, in these close to 1:1 atomic ratio alloys, is shifted to higher binding energies. We think that only some small part of the density of 3d states can survive at E_F, after the charge transfer mentioned above, but this appears to be quite enough to maintain a relatively large 5f-3d hybridization, which becomes responsible mostly for a nonmagnetic ground state of uranium atoms in UFeAl. From such a picture, among others, one may infer, e.g., the relatively low γ value found for UFeAl [$\gamma(0) = 25$ mJ mol^{-1} K^{-2}].[1] Nevertheless, this compound is on the verge of the appearance of magnetism. As Fig. 2 illustrates, the susceptibility increases

rapidly at low temperatures, when the process of Fe atom substitution by Ni in the alloy starts to take place. From the Mössbauer-effect studies we know that it initially happens mainly in the (1b) sites, i.e., around the location of the uranium atom. In view of the magnetic properties, the vicinity of a magnetic ion plays the key role. In fact, this atomic interexchange gives rise to the development of local magnetic correlations, which in turn yield a small deviation from the randomness of the atomic arrangements, and consequently lead to a local short-range magnetic order or/and cluster glass formation. They are just responsible for a noncollinear field dependence of the magnetization for the samples with $x \geq 0.2$. At the same time, the lattice parameter a, which determines both the closest U-U and U-Fe(1b) distances in the basal plane, continuously increases until reaching the composition $x \approx 0.35$ (see Fig. 5). Also the number of conduction electrons rises rapidly with the Ni substitution. Consequently, all these facts lead to a reduction of the degree of 5f-3d hybridization. In turn, the latter implies the reducing also of the conduction-electron–f-electron exchange interaction parameter J_{cf} according to the proportionality (see Refs. 14 and 15)

$$J_{cf} \approx V_{cf}^2 / (E_F - E_f) \, , \tag{1}$$

where V_{cf} is the hybridization matrix element and E_f is the position of the 5f level relative to the Fermi energy E_F. In the above expression, the V_{cf} value changes with the variation of both the number of total electrons and the U-Fe(1b) distance, while the position E_f with respect to E_F, is rather constant, due to a strong pinning of the f level to E_F.[16]

A more detailed consideration of the process described above has very recently been given by Endstra, Nieuwenhuys, and Mydosh[15] who reported a hybridization model allowing the determination of magnetic ordering trends in the intermetallic 1:2:2 compound series of uranium and cerium. For example, in this model the hybridization, which is solely determined by the degree of the d-band filling, and thus the calculated value of V_{df} matrix elements, increases in the following order: Cu$\rightarrow$Ni$\rightarrow$Co$\rightarrow$Fe. Hence, e.g., UFe$_2$(Si,Ge)$_2$, which shows also the exchange-enhanced Pauli paramagnetism [χ(RT) = (3–4) $\times 10^{-3}$ emu/mol],[17,18] as does UFeAl, possess the largest V_{df} values among the 3d series of 1:2:2 compounds.[15] A simple comparison of UFeAl to UFe$_2$(Si,Ge)$_2$ shows that for the latter compounds the U/Fe atomic ratio is different by a factor of 2 and thus more electrons are needed to fill up the 3d band. We conclude that the 5f-3d hybridization should be even stronger for them than in the case of UFeAl.

Bearing all these facts in mind, we see that the development of the long-range ferromagnetism in the composition range of $0.35 \leq x \leq 0.8$ in the UFe$_{1-x}$Ni$_x$Al system, and the bell shape of the T_C vs x curve with the maximum $T_C = 55$ K at $x = 0.5$, could now be easily accounted for by the concept of the $T = 0$ K magnetic phase diagram of the Kondo lattices, developed by Doniach[19,20] as is the case of 1:2:2 uranium intermetallic compounds. This diagram says that when the exchange coupling in-

tegral J decreases below its critical value J_{cr} a long-range magnetic order occurs in a system at T_C which passes through a maximum and then tends slowly to zero value with further decreasing J, if, of course, another mechanism of magnetic exchange (e.g., superexchange) does not start to play a dominant role due to the vanishing of the hybridization phenomenon. Therefore, the occurrence of antiferromagnetism for the compositions with $x \geq 0.9$, and further for UNiAl (Ref. 3), should be treated in a somehow different manner. It is well known that this kind of magnetic-moment coupling is characteristic for a number of similar uranium ternary compounds based on Pd, Cu, and Au, for which the degree of $5f$-ligand hybridization is commonly regarded as the lowest one.

Finally, one should pose the question whether we are dealing in such a system with $3d$ magnetism as well. At a first glance the $3d$ electrons seem to be magnetically inactive. However, a final solution of this question can be done on the basis of polarized neutron-diffraction studies. For example, for isostructural UCoAl, such studies have revealed that besides the uranium the cobalt atoms also carry magnetic moments of about $0.06\mu_B$.[21]

ACKNOWLEDGMENT

---

*Permanent address: Physicotechnical Institute, Russian Academy of Sciences, 420029 Kazan, Sybirski Trakt 10/7, Russia.

[1]V. Sechovsky and L. Havela, in *Ferromagnetic Materials,* edited by E. P. Wohlfarth and K. H. J. Buschow (North-Holland, Amsterdam, 1988), p. 309, and references therein.

[2]R. Troć, V. H. Tran, F. G. Vagizov, and H. Drulis, J. Alloys Compounds **200**, 307 (1993).

[3]V. Sechovsky, L. Havela, F. R. de Boer, J. J. M. Franse, P. A. Veenhuizen, J. Sebek, J. Stehno, and A. V. Andreev, Physica B **141**, 283 (1986).

[4]J. M. Fournier and P. Burlet (unpublished).

[5]L. Havela, V. Sechovsky, P. Nozar, E. Brück, F. R. de Boer, J. C. P. Klaase, A. A. Menovsky, J. M. Fournier, M. Wulff, E. Sugiura, M. Ono, M. Date, and A. Yamagishi, Physica B **163**, 313 (1990).

[6]E. Brück, F. R. de Boer, P. Nozar, V. Sechovsky, L. Havela, K. H. Buschow, and A. V. Andreev, Physica B **163**, 378 (1990).

[7]T. Gasche, S. Auluck, M. S. S. Brooks, and B. Johansson, J. Magn. Magn. Mater. **104&107**, 37 (1992).

[8]L. Havela, T. Almeida, J. R. Naegale, V. Sechovsky, and E. Brück, J. Alloys Compounds **181**, 205 (1992).

[9]J. Schoenes, F. Troisi, E. Brück, and A. A. Menovsky, J. Magn. Magn. Mater. **108**, 40 (1992).

[10]V. Sechovsky, L. Havela, J. Jirman, E. Brück, F. R. de Boer, H. Nakotte, W. Ye, T. Takabatake, H. Fujii, T. Suzuki, and

T. Fujita, Physica B **177**, 155 (1992).

[11]I. M. Reznik, F. G. Vagizov, and R. Troć, following paper, Phys. Rev. B **51**, 3013 (1995).

[12]J. J. M. Franse, P. H. Frings, F. R. de Boer, and A. Menovsky, in *Physics of Solids Under High Pressure,* edited by J. S. Schilling and R. N. Shelton (North-Holland, Amsterdam, 1981), p. 181.

[13]A. Grassmann, Physica B **163**, 547 (1990).

[14]E. W. Scheidt, H. Riesemeier, K. Lüders, M. Robrecht, and J. Hasse, J. Alloys Compounds **183**, 116 (1992).

[15]T. Endstra, G. J. Nieuwenhuys, and J. A. Mydosh, Phys. Rev. B **48**, 9595 (1993).

[16]B. Wieslau and N. Grewe, Physica B **165&166**, 387 (1990).

[17]A. Szytula, S. Siek, J. Leciejewicz, A. Zygmunt, and Z. Ban, J. Phys. Chem. Solids **49**, 1113 (1988).

[18]A. J. Dirkmaat, T. Endstra, K. A. Kuetsch, A. A. Menovsky, G. J. Nieuwenhuys, and J. A. Mydosh, J. Magn. Magn. Mater. **84**, 143 (1990).

[19]S. Doniach, in *Valence Instabilities and Related Narrow Band Phenomena,* edited by R. D. Parks (Plenum, New York, 1977), p. 169.

[20]S. Doniach, Physica B **91**, 231 (1977).

[21]M. Wulff, J. M. Fournier, A. Delapalme, B. Gillon, V. Sechovsky, L. Havela, and A. V. Andreev, Physica B **163**, 331 (1990).